Schweizerischer Erdbebendienst
Service Sismologique Suisse
Servizio Sismico Svizzero
Swiss Seismological Service

An efficient hybrid SBI-FD numerical framework for modeling fluid migration and fault-fluid interactions

Yu-Han Wang [1] Elias Rafn Heimisson [1,2]

[1]Swiss Seismological Service, ETH Zurich, Zurich, Switzerland [2]Institute of Earth Sciences, University of Iceland, Reykjavik, Iceland

ETH zürich

Background

- The modeling and prediction of fault structure/gouge **localization** are crucial for understanding **earthquake origins** because localization initiates fault slip, thereby necessitating the development of an efficient numerical scheme.
- **Continuum methods** encounter significant challenges due to the substantial increase in computational resources required as the model size expands.
- **Boundary integral methods** struggle with accurately describing material heterogeneity, a common characteristic of the bulk.

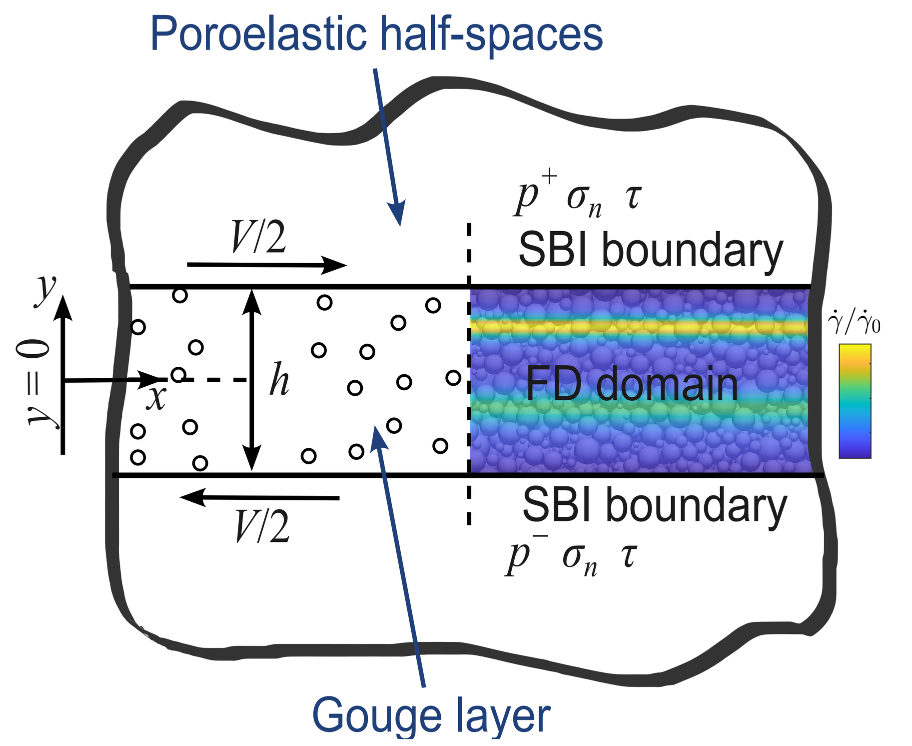

Figure 1. Schematic overview of the problem we aim to model. A gouge layer with a finite thickness h experiences the shearing between two rigid poroelastic bulks with a velocity V relative to each other (see Fig. left). The localization of strain, pore pressure, and so on can be the result per see (see Fig. right).

The SBI-FD framework for fluid diffusion in fault structures

Before exploring the development of models that account for fault-fluid interactions, our initial focus is on fluid diffusion within fault structures. As depicted in the schematic below, we specifically divide the model into three subdomains:

- **The host rock.** The domain is truncated by the SBIM. The permeability is isotropic.
- **The damage zone.** The domain is simulated with the FDM. The permeability is anisotropic.
- **The fault core.** The domain is simulated with the FDM. The permeability is anisotropic.

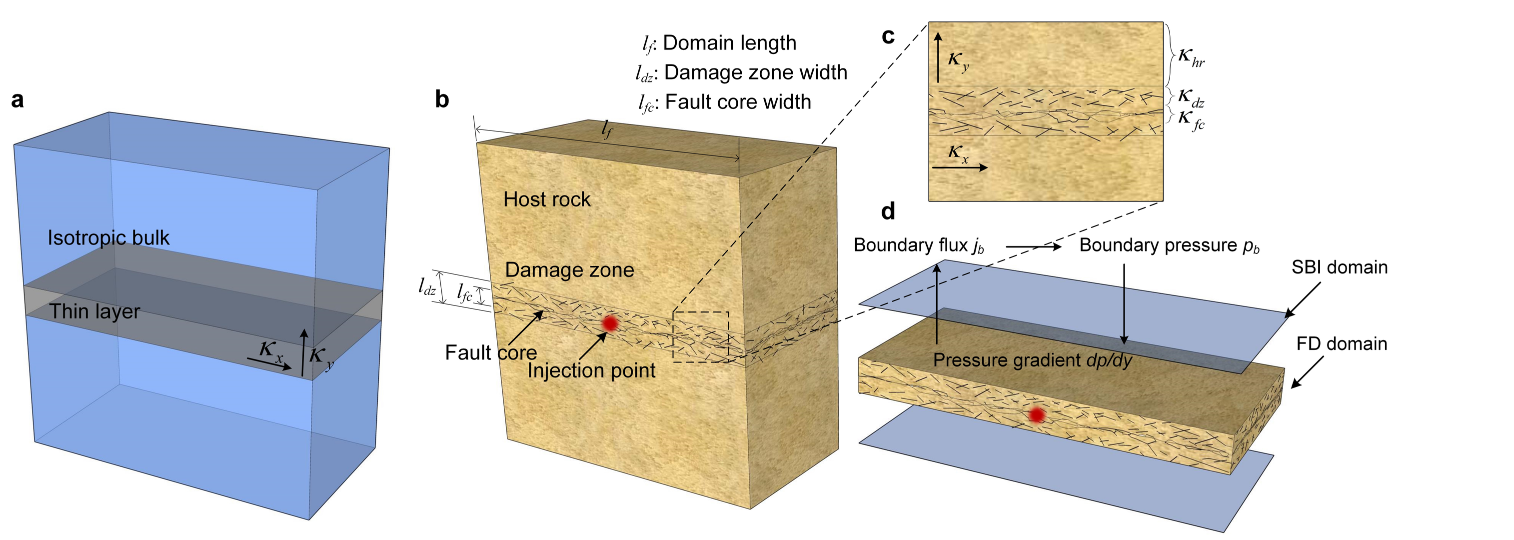

Figure 2. Problem Setup: (a) Schematic of the generalized problem. (b) Schematic of a fault structure and host rock with heterogeneous mobility. The injection point is marked by the red dot, which can be located in either the fault core or damage zone. (c) The mobility symbols in each domain, where κ_x and κ_y represent the mobility along the x and y directions, respectively. Additionally, κ_{hr}, κ_{dz}, and κ_{fc} represent the mobility of the host rock, damage zone, and fault core, respectively. (d) The SBI-FD coupling cycle for the fault structure consists of the boundary flux calculation and the boundary pressure resolved with the SBIM.

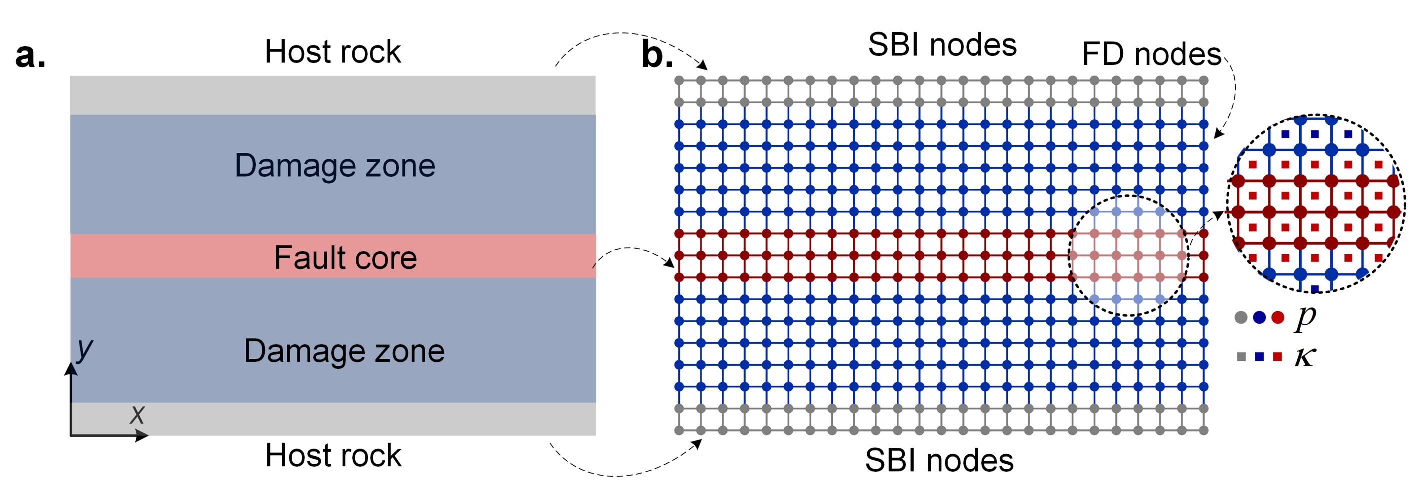

Figure 3. (a) This 2D diagram illustrates the sub-components of our fault model. The host rock is depicted in gray, while the blue region represents the damage zone. The central light red band corresponds to the fault core. These areas differ in terms of their permeability properties, specifically their mobility (κ_{hr}, κ_{dz} and κ_{fc}, as shown in Fig. 2c). (b) In the context of the conservative finite difference scheme, this diagram illustrates our grid configuration. The rectangles indicate mobility nodes, while circular grids are used to address pressure. We apply Dirichlet's boundary conditions, setting the pressure to zero at both bilateral boundaries for our model. Note that only the boundary layer of the host rock is solved by the SBIM, while the other layer is by the FDM to ensure stability.

Model benchmark (SBI-FDM versus FDM)

To cover broader and generalized scenarios, we have undertaken verification of the method against a **heterogeneous** medium. Here, three injection points are positioned within the damage zone, maintaining a consistent spacing of one-third of the fault length $l_f/3$ along the fault length. A constant injection rate is fixed initially for time t_0. After that, the injection stops and the fluid continues migrating in the fault.

The relationship between injection rate and time is expressed as:

$$V_f(t) = \begin{cases} \Phi t & \text{if } t < t_0 \\ \Phi t_0 & \text{if } t \geq t_0 \end{cases}. \tag{1}$$

The injection time $t_0 = 1500s$ in this case.

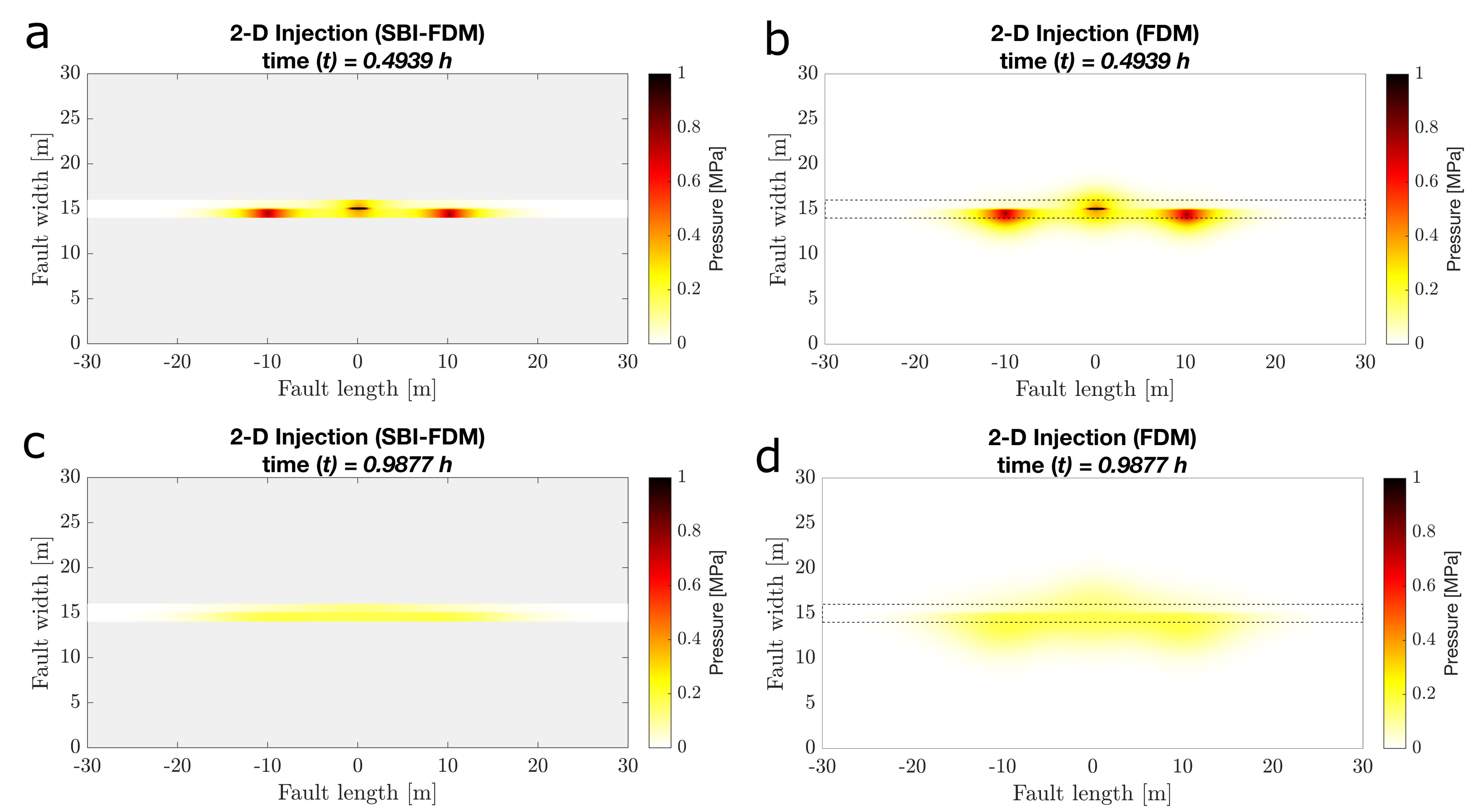

Figure 4. Pressure profiles during fluid migration, as resolved by the SBI-FDM, in heterogeneous fault structures, compared to the FDM: (a) and (b) at approximately $t \approx 0.5$ h; (c) and (d) at approximately $t \approx 1$ h. The gray areas represent the bulk, excluded from modeling with the SBI-FDM.

Computational efficiency demonstration

We compare the speed of the **FD and SBI-FD** methods. Two specific comparison tests are designed and depicted in the inset of figures below, where l_f represents the length of the original domain, and l_f' denotes the length after scaling. Initially, the domain is shaped as a cube with the fault structure centrally positioned within it.

Despite the inset figures may seem homogeneous, it is noted that the fault structure consists of the fault core and the damage zone with a layered formation, which is widely used in testing the performance of hybrid methods.

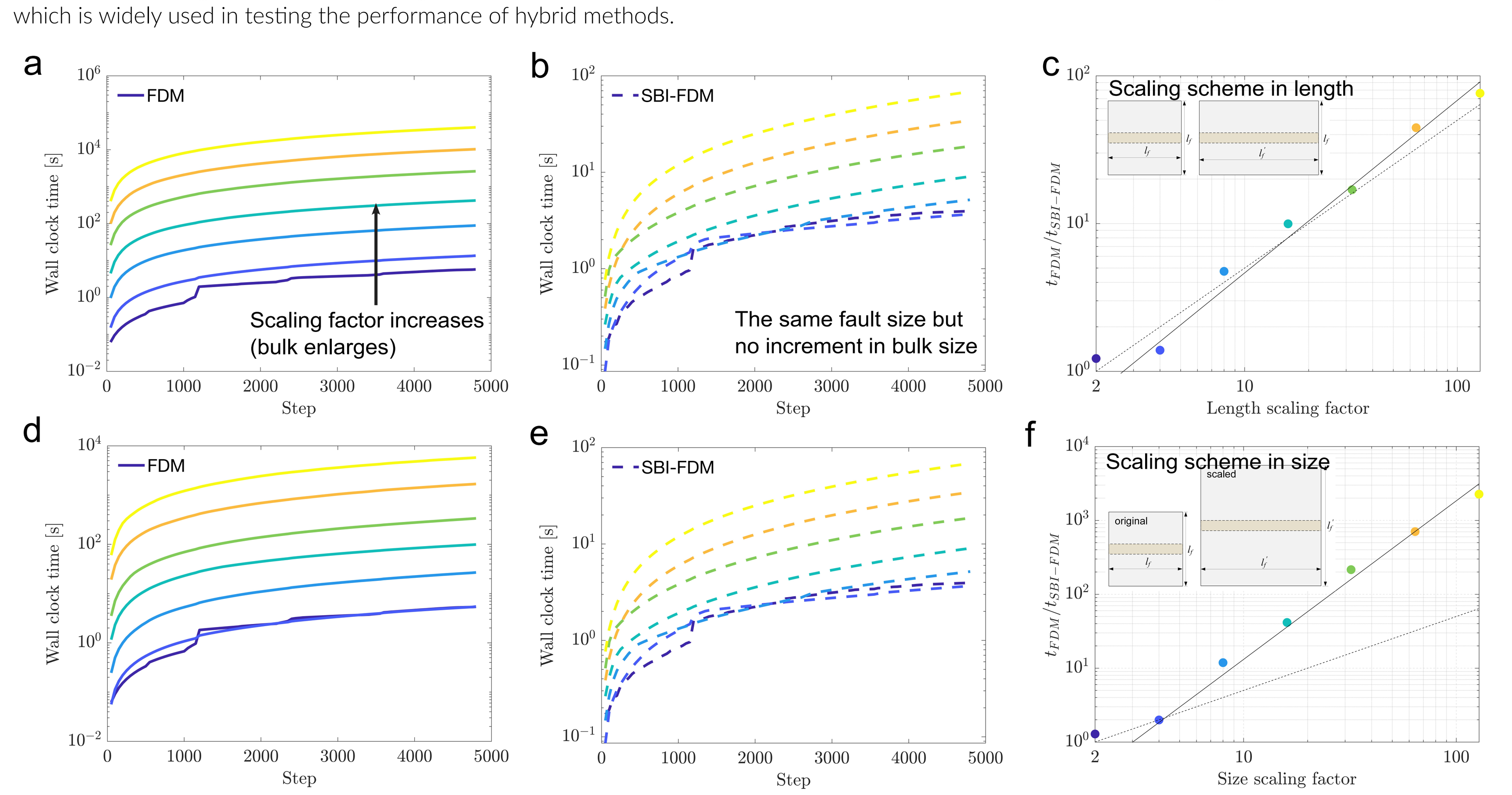

Figure 5. Wall clock times used for computation are presented as follows: (a) FD cases with scaling along the length. The length scaling factor ranges from one to seven with an interval of one, as shown in response to the inset of the right figure. (b) SBI-FD cases with a length scaling factor ranging from one to seven. (c) Speedup versus the length scaling factor. (d) FD cases with scaling along the size. The size scaling factor remains consistent with that of the length. (e) SBI-FD cases with a size scaling factor ranging from one to seven (the same as b). (f) Speedup versus the size scaling factor. The dashed reference line represents a linear relation with a proportionality coefficient of one. The solid line is a linear fit of the remaining data points, excluding the case with the minimum scaling factor.

Incorporation of poroelasticity

Inheriting the SBI-FD framework, we further extend the model to regard the **interactions between fluids and fault slip**.

Governing equations

Constitutive relationship

Frictional law

$$f(\dot{\gamma}) = (a-b)\sinh^{-1}[\frac{\dot{\gamma}}{2\dot{\gamma}_0}\exp(\frac{f_0}{a-b})] \tag{2}$$

Mechanical equilibrium

$$\frac{\partial \tau}{\partial y} = 0, \frac{\partial \sigma_n}{\partial y} = 0, \tau = f(\sigma_n - p) \tag{3}$$

Conservation equations

Conservation of energy

$$\frac{\partial T}{\partial t} = \frac{\tau\dot{\gamma}}{\rho c} + \alpha_{th}(\frac{\partial^2 T}{\partial x^2} + \frac{\partial^2 T}{\partial y^2}) \tag{4}$$

Conservation of pore fluid

$$\frac{\partial p}{\partial t} = \Lambda\frac{\partial T}{\partial t} - \frac{\epsilon}{\beta\dot{\gamma}}\frac{\dot{\gamma}}{t} + \alpha_{hy}(\frac{\partial^2 p}{\partial x^2} + \frac{\partial^2 p}{\partial y^2}) \tag{5}$$

Note: The current model is developed under a pseudo-2D condition in regard to mechanical equilibrium equations, i.e. the normal stress along the fault length is not considered.

Localization inside the fault incorporating poroelasticity

We initialize the gouge shearing model with a beginning velocity $V_0 = 1$m/s and the velocity is updated by the integration of $\dot{\gamma}$ across the fault thickness.

$t = 0.0060000\,\mathrm{s}$, $\sigma_{xz,0} = 75.60\,[\mathrm{MPa}]$, $\sigma_{n,0} = 0.00\,[\mathrm{MPa}]$, $\dot{\gamma}_0 = 1000.00000\,[1/\mathrm{s}]$

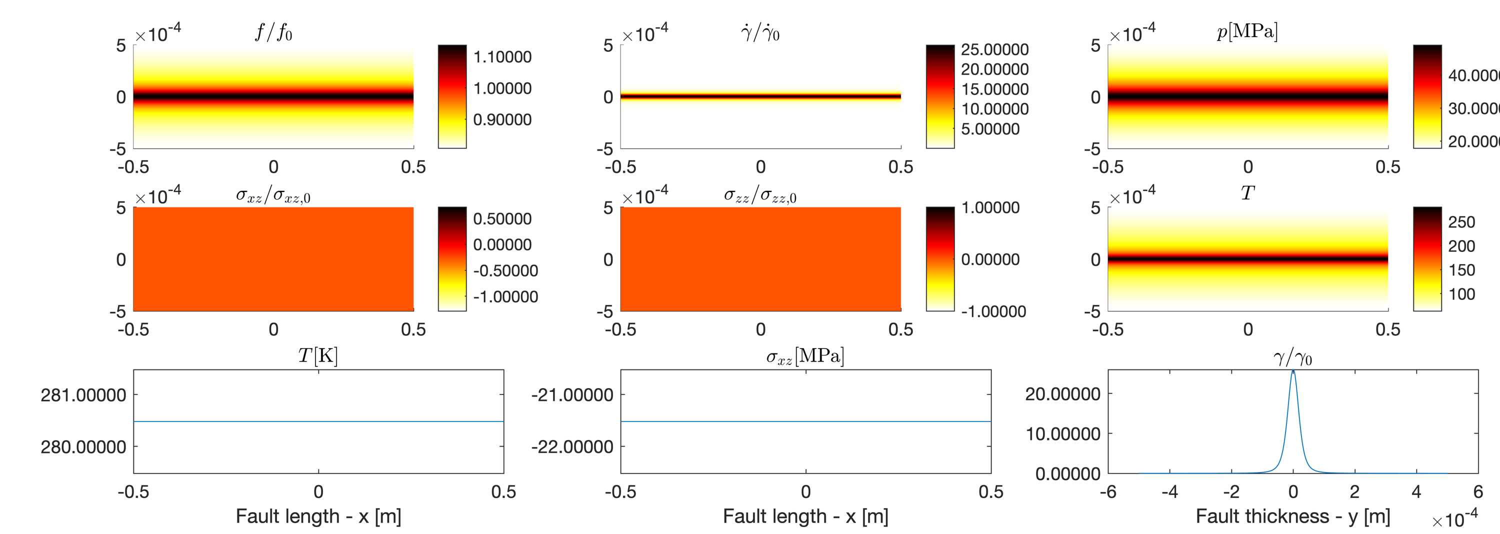

Figure 6. The parameter field after localization happens. In the first row, from left to right, we present the normalized frictional coefficient f/f_0 field, the normalized shear strain rate $\dot{\gamma}/\dot{\gamma}_0$, and the pore pressure. As of the second row, from left to right, we have shear stress and normal stress fields, and temperature, accordingly. For the third row, we take the section of the temperature field and shear stress along the fault length to check the pseudo-1D condition. In the bottom right corner, the shear strain rate across the gouge is plotted to show the localized shear strain rate pattern.

Conclusions and follow-up works

- We show the SBI-FD scheme **agrees well** with the FDM solution and is in possession of convergence stability.
- The SBI-FD method shows privilege in **relieving computational resources' consumption** compared with continuum methods.
- The gouge shearing model established with the **poroelastic** SBI-FD method can reproduce the **localization** during fault slip.

Follow-up works:

- Integration of heterogeneous and anisotropic gouge permeability/initial pore pressure to see if they are crucial to the localizing evolution.
- Comparison with laboratory/field observation (localization pattern + fault slip distance).

Acknowledgements

We would like to thank the Swiss National Science Foundation for supporting this research through the Ambizione grant number PZ00P2 208993.

Selected references

[1] John D Platt, John W Rudnicki, and James R Rice. Stability and localization of rapid shear in fluid-saturated fault gouge: 2. localized zone width and strength evolution. *Journal of Geophysical Research: Solid Earth*, 119(5):4334–4359, 2014.

[2] Yuhan Wang and Elias Rafn Heimisson. A coupled finite difference-spectral boundary integral method with applications to fluid diffusion in fault structures. *International Journal for Numerical and Analytical Methods in Geomechanics*, 2024.

Sharing is encouraged

Check here: the QR code links to an implementation of the SBI-FD model of our latest paper recently accepted in *International Journal for Numerical and Analytical Methods in Geomechanics.*

yuhan.wang@sed.ethz.ch